Ground and Low-Lying Excited Electronic States of Difluorodiazirine†

Rajeev R. Pandey,‡ Yuriy G. Khait,§ and Mark R. Hoffmann*

Chemistry Department, University of North Dakota, Grand Forks, North Dakota 58202-9024

Received: October 15, 2003; In Final Form: January 12, 2004

Ground and low-lying excited electronic states of difluorodiazirine (F_2CN_2) were investigated using the recently revised, multireference, second-order generalized Van Vleck perturbation theory (GVVPT2). Initial studies on the ground state were carried out with the single-reference Møller−Plesset second order perturbation theory (MP2), quadratic configuration interaction with single and double excitation (QCISD), and coupled cluster with single, double, perturbative triple excitations (CCSD(T)) methods using several correlation-consistent atomic basis sets. MP2 and QCISD did not give semiquantitatively correct descriptions of the ground state of the molecule. For the ground state, GVVPT2 results are in close agreement with CCSD(T) but lie slightly closer to the experimental results. A balanced treatment of nondynamic and dynamic correlation effects has been shown to be of crucial importance for correct description of the system. Equilibrium geometries, excitation energies, and thermodynamic stabilities of the states were calculated and compared with available experimental data. It has been shown for the first time that not only is the ground-state metastable but that the lowest excited state (1^3B_1) is also metastable, relative to decay into CF_2 and N_2; this may be important to elucidating the mechanism of ultraviolet photolysis of this compound.

1. Introduction

The main structural feature of diazirines is their three-membered CN_2 rings. In contrast to the parent diazirine, H_2CN_2, which is thermodynamically stable relative to $CH_2 + N_2$ and has a significant dipole moment (1.57 D),[1] difluorodiazirine (F_2CN_2) is energetically higher lying[2] than its dissociation products ($CF_2 + N_2$) and seems to have an almost vanishing dipole moment.[3] Structurally, difluorodiazirine has a longer N−N bond length (by 0.07 Å) and a shorter C−N bond length (by 0.06 Å) than those in H_2CN_2 (see discussion and refs in ref 4). The ground-state potential-energy surface of CF_2N_2 is scantily characterized; of all seven plausible isomers, only two, difluorodiazirine and difluorocyanamide ($F_2NC{\equiv}N$), are experimentally known.

Much of the interest in the chemistry of difluorodiazirine arises from its use as an effective precursor of the singlet difluorocarbene diradical, F_2C**:**, which is actively used for the stereospecific difluoromethylenation of olefins.[5,6] This diradical is produced from difluorodiazirine by ultraviolet photolysis (or by pyrolysis).[5,7] Although molecular properties of difluorodiazirine have been the subject of a number of experimental investigations (see refs 3 and 8−19, and refs therein) and it is known that its photolysis involves excited electronic state(s), little is known about the low-lying excited states of the molecule. Herein, we address the results of the first theoretical study of such states.

The most recent ab initio calculations of the molecule, performed by Boldyrev et al. at the MP4//MP2/6-31G* level, showed that difluorodiazirine is more stable than its cyanamide isomer (by about 68 kcal/mol), although it is energetically metastable (by 28.9 kcal/mol) relative to decay into $CF_2 + N_2$.[2] The barrier preventing such decay was predicted to be about 34 kcal/mol. Although these results agree with the experimental observations that difluorocyanamide is a highly explosive compound and can easily rearrange to difluorodiazirine at room temperature (in the presence of a CsF catalyst),[20] the MP level of theory can only be expected to be qualitatively correct. Even then, the MP level of theory is only applicable to the ground state of molecules with three-membered rings,[21−23] which may be single-determinant dominated, and not their excited states.[22] The theoretical investigation of such states is a significant computational challenge and requires using high-level methods that ensure a balanced treatment of dynamical and nondynamical electron correlation. With this aim, in the present work we used the recently revised, second-order generalized Van Vleck perturbation theory[24−26] (GVVPT2) variant of multireference perturbation theory. GVVPT2 has proved to be sufficiently accurate in describing the excited states of the closely related difluorodioxirane molecule[22] (F_2CO_2) and other difficult molecular systems (see, e.g., ref 27). In general, GVVPT2 provides a balanced treatment of dynamical and nondynamical correlation effects and gives results in close agreement with coupled cluster with single, double, perturbative triple excitations (CCSD(T)) (when it is applicable) and even proves to be a useful alternative to MRCISD.

Experimental data for F_2CN_2 are mainly limited to its $\tilde{X}^1A_1$ ground state and to the $\tilde{A}^1B_1$ lowest singlet excited state, involved in the photolysis of the molecule.[15,16] In both states, the molecule has C_{2v} symmetry. The geometry of the ground state has been determined[12] from an electron-diffraction study.[8] The only structural data known about $\tilde{A}^1B_1$ are the estimated values of the change in R_{NN} and R_{FF} as a result of electronic excitation.[15] Fundamental vibrational frequencies in both states have been obtained from combined analysis of infrared,[18] Raman,[19] and UV spectra.[3,11−17] The origin of the $\tilde{A}^1B_1 \leftarrow \tilde{X}^1A_1$

† Part of the special issue "Fritz Schaefer Festschrift".

* Author to whom correspondence may be addressed. Email: mhoffmann@chem.und.edu.

‡ Present address: Department of Electrical Engineering, University of California, Riverside, CA 92521.

§ Permanent address: 14 Dobrolyubova Ave., Russian Scientific Center "Applied Chemistry", St. Petersburg 197198, Russia.

10.1021/jp0311658 CCC: $27.50
Published on Web 02/13/2004

TABLE 1: Comparison of Theoretical and Experimental Geometries (Å and deg) of Ground State F_2CN_2 ($\tilde{X}^1A_1$)

	cc-pVDZ			cc-pVTZ			aug-cc-pVDZ		aug-cc-pVTZ		
	MP2	QCISD	CCSD(T)	MP2	QCISD	CCSD(T)	MP2	QCISD	MP2	QCISD	exp[a]
R_{NN}	1.307	1.280	1.290	1.296	1.268	1.280	1.312	1.282	1.295	1.267	1.293(9)
R_{CN}	1.412	1.411	1.416	1.405	1.401	1.410	1.416	1.413	1.405	1.401	1.426(4)
R_{CF}	1.333	1.332	1.334	1.326	1.322	1.326	1.346	1.343	1.328	1.324	1.315(4)
∠NCN	55.1	53.9	54.2	54.9	53.8	54.0	55.2	54.0	54.9	53.7	54.00(36)
∠FCF	110.7	110.7	110.7	110.7	110.6	110.7	110.5	110.5	110.7	110.6	111.80(52)

[a] Reference 8.

TABLE 2: Comparison of GVVPT2-Optimized Geometries (Å and deg) of Ground State F_2CN_2, Using Different Model Spaces and Basis Sets, with Experiment[8]

	cc-pVDZ						cc-pVTZ		
	{3,3,4}{5}	{5}{5}	{4}{6}	{6}{6}	{14}{6}	{4}{5}	{4}{5}	{6}{6}	exp
R_{NN}	1.288	1.300	1.292	1.291	1.287	1.294	1.281	1.288	1.293(9)
R_{CN}	1.421	1.410	1.423	1.415	1.413	1.423	1.417	1.399	1.426(4)
R_{CF}	1.332	1.348	1.322	1.347	1.344	1.326	1.319	1.340	1.315(4)
∠NCN	53.9	54.9	54.0	54.3	54.2	54.1	53.7	54.8	54.00(36)
∠FCF	110.6	110.6	111.4	110.2	110.0	111.4	111.2	110.4	111.8(52)

electronic transition has been located at 28 374.2 cm^{-1}.[12,15] The minimum of the lowest triplet state (presumably 1^3B_1) has been evaluated to be ca. 7200 cm^{-1} below the minimum of the $\tilde{A}^1B_1$ state.[11] Although $\tilde{A}^1B_1$ is known to predissociate slowly even in its 0° level,[16] the mechanism of the predissociation is still unknown.

In the present work, equilibrium geometries, thermodynamic stabilities, and vertical and adiabatic excitation energies of the ground and lowest excited singlet and triplet states of each symmetry of F_2CN_2 (i.e., $1,2^1A_1$, $1^{1,3}B_1$, $1^{1,3}B_2$, and $1^{1,3}A_2$) have been studied using GVVPT2 and the cc-pVDZ and cc-pVTZ basis sets. Additional studies of the ground state were performed using standard Møller−Plesset second order perturbation theory (MP2), quadratic configuration interaction with single and double excitation (QCISD), and CCSD(T) methods and additional (augmented) basis sets. The paper begins with a brief review of the GVVPT2 approach, a description of computational details, and an analysis of the applicability of the used methods for studying the ground state of the molecule. The electronic nature of the excited states, their predicted molecular properties, and comparison with available experimental data are discussed in section 3. In the last part of section 3, we evaluate thermodynamic stabilities of the lowest excited states and discuss a possible role of the 1^3B_1 state in the predissociation of the $\tilde{A}^1B_1$ term. A final section summarizes the results of the present work.

2. Assessment of Methods and Computational Details

The current implementation of the GVVPT2 method has been described in detail elsewhere.[24] Here we only mention salient features of the method. GVVPT2 is both state selective (more precisely, subspace selective) and of the "perturb-then-diagonalize" variant of quasidegenerate perturbation theory (QDPT), whose basic formulas are well-defined approximations to the theoretically solid SC-QDPT approach.[28] In GVVPT2, a model configuration space, which is usually spanned by the configuration state functions (CSF) used to construct the MCSCF functions, is partitioned into a primary subspace, involving the lowest states of physical interest and its orthogonal complement (the secondary subspace). Excited configurations, connected with the model ones through one- and two-electron excitations, span an external space. Unlike most multireference perturbation theories, GVVPT2 takes into account the interactions of the perturbed primary states with the (unperturbed) secondary states and thus allows for the effects of dynamic electron correlation on the nondynamical part. The method is not subject to the intruder state problem and leads to smooth potential-energy surfaces even when surfaces are in close proximity. GVVPT2 does not impose any restrictions on the structure of the model space, and this flexibility of the method has been actively used in our GVVPT2 program[24] through use of the recently developed macroconfiguration approach.[29] The program gives the possibility to use physical considerations in constructing truncated model spaces and to consider efficiently large external configuration spaces. All these advantages of the GVVPT2 method are relevant to the present work.

To investigate the applicability of different methods for the description of the ground-state geometry of difluorodiazirine, we performed optimizations at the MP2, QCISD, CCSD(T), and GVVPT2 levels with several basis sets. Specifically, GVVPT2 and CCSD(T) optimizations have been performed using correlation-consistent, polarized basis sets (i.e., cc-pVDZ and cc-pVTZ), while MP2 and QCISD calculations have been carried out using these bases and additionally the augmented cc-pVDZ and cc-pVTZ sets. MP2, QCISD, and CCSD(T) calculations were performed using the Gaussian 98 suite of programs.[30]

Comparison of structural parameters of the molecule, predicted by the MP2, QCISD, and CCSD(T) methods, with the results of electron-diffraction measurements[8] are given in Table 1. For all considered basis sets, the MP2 and QCISD methods predict almost the same values for structural parameters (excepting the N−N bond), which are not in good agreement with experiment. At the QCISD/aug-cc-pVTZ level, the C−N bond length is predicted to be 0.025 Å too short and the C−F bond length is predicted to be 0.009 Å too long. Predictions of the N−N bond length vary widely between MP2 and QCISD, and although the MP2 results are close to experiment for cc-pVTZ and aug-cc-pVTZ basis sets, the large deviation of QCISD results from experiment (−0.026 Å) suggests that the MP2 results are fortuitous. Table 1 shows also that even the higher-correlated CCSD(T) method, with cc-pVTZ basis, does not lead to a quantitatively correct description of the bond lengths in this molecule.

GVVPT2 geometries of the F_2CN_2 ground state, optimized with several basis sets and model spaces, are compared with experiment[8] in Table 2. Model spaces denoted as $\{n_o\}\{n_v\}$ include all spin and space symmetry allowed configurations generated by single and double excitations from the n_o highest

occupied orbitals to the n_v lowest unoccupied orbitals. MCSCF calculations for the ground state within such model spaces were performed using the MCSCF program described in ref 31. Our preliminary, single-reference studies of the ground state showed that the group of the 10 highest occupied orbitals is naturally divided into three subgroups involving three, three, and four orbitals, respectively ($\{n_o = 10\} = \{3,3,4\}$). The first subgroup includes the three lowest orbitals, $G_1 = (6a_1, 7a_1, 2b_2)$, which are mainly 2s atomic orbitals localized on the carbon and nitrogen atoms; the second one includes the three higher-lying orbitals, $G_2 = (1a_2, 4b_1, 3b_2)$, describing bonds within the CF_2 fragment; and finally, the third subgroup includes the four highest occupied bonding orbitals, $G_3 = (8a_1, 9a_1, 5b_1, 4b_2)$, localized on the CN_2 ring. The five lowest virtual orbitals, $\{n_v = 5\} = (10a_1, 2a_2, 6b_1, 5b_2, 6b_2)$, are also mainly localized within the CN_2 ring. On the basis of such partitioning of the high-lying occupied and low-lying unoccupied orbitals, we considered one more model space, designated in Table 2 as {3,3,4}{5}, which was created by eight macroconfigurations describing single and double excitations from the groups G_1, G_2, and G_3 to the virtual group.

As mentioned in the overview of GVVPT2, the external space is generated from all single and double excitations from the model space configurations, except that we chose to restrict the 1s-like lowest-lying orbitals to be doubly occupied in all configurations. Note that all "internal" single and double excitations that were not included in the model space and all single and double "semi-internal" excitations were included in the GVVPT2 calculations.

Table 2 demonstrates that GVVPT2 results are sensitive to the choice of model space, which corroborates the earlier observation that a balanced treatment of dynamical and nondynamical correlation effects is critically important for the correct description of even the ground state of F_2CN_2. Taking into account the localized character of the occupied and unoccupied orbitals used in constructing model spaces, it is not surprising that the {4}{5} model space produces the most satisfying results, in terms of cc-pVTZ results agreeing best with experiment and in terms of cc-pVDZ and cc-pVTZ results agreeing with CCSD(T). In this case, we take into account variationally only the lowest-energy excitations localized within the CN_2 ring, while all other excitations (in particular, the essentially higher energy excitations from the CF_2 fragment to CN_2) are described perturbatively, along with other high-energy excitations.

Taking these results into account, we have optimized the geometries of excited states using the {4}{5} model space with the cc-pVDZ basis set, while more accurate vertical and adiabatic excitation energies of the states have been calculated using the cc-pVTZ basis. As will be shown in the next section, in the case of the $\tilde{A}^1B_1$ state where experimental data are available, such an approach describes quite well changes in the geometry of the molecule caused by electron excitations and moreover leads to good agreement with experimental data for the vertical excitation energy of the state.

The {4}{5} model space is determined by the three model macroconfigurations: ... $(G_3)^8(G_v)^0$, ... $(G_3)^7(G_v)^1$, and ... $(G_3)^6(G_v)^2$ and, in the case of the ground state, was spanned by 67 CSF of $^1A_1$ symmetry (created by 51 configurations). The dimension of the corresponding external space depended strongly on the atomic basis and was rather large. In the case of cc-pVDZ, the external space was spanned by 23 075 702 CSF (3 765 215 configurations), whereas in the case of the cc-pVTZ set, its dimension increased to about 166.5 million CSF (more than 26 million configurations). Although the dimensions of the model spaces were almost the same for all the considered states and the dimensions of the external spaces for the singlet excited states remained close to that for the ground state, the dimensions of the triplet spaces increased significantly (e.g., 43.2 million CSF for cc-pVDZ).

TABLE 3: GVVPT2/cc-pVDZ-Optimized Geometries (Å and deg) of the Excited States of F_2CN_2 Studied in the Present Work.

	1^1B_1	1^3B_1	1^1B_2	1^3B_2	1^1A_2	1^3A_2	2^1A_1
R_{NN}	1.325	1.318	1.751	1.645	1.687	1.572	1.423
R_{CN}	1.462	1.479	1.399	1.424	1.406	1.416	1.450
R_{CF}	1.304	1.303	1.350	1.325	1.347	1.342	1.287
R_{FF}	2.148	2.155	2.191	2.201	2.165	2.166	2.104
∠NCN	53.9	52.9	77.4	70.5	73.7	67.4	58.8
∠FCF	110.8	111.6	108.5	112.4	107.0	107.6	109.7

Our GVVPT2 calculations showed that the ground state of difluorodiazirine had two configurations with large amplitudes; the leading configuration $...(8a_1)^2(9a_1)^2(5b_1)^2(4b_2)^2(2a_2)^0$ had an amplitude of 0.89, and the second-largest model configuration, $...(8a_1)^2(9a_1)^2(5b_1)^0(4b_2)^2(2a_2)^2$, had an amplitude of 0.14. These configurations are related through the double excitation from the π-bonding N−N orbital ($5b_1$) to the π-antibonding N−N orbital ($2a_2$). Note that, at the MCSCF level, the amplitude of the leading configuration was essentially larger (0.969) than at the GVVPT2 level (while the amplitude of the second configuration was almost the same (0.15)). This demonstrates the large effect of dynamic correlation on the configuration structure of even the ground state of the molecule. The same effect has been observed for the excited states.

3. Molecular Properties and Nature of Excited States

The geometries of all the low-lying excited states considered in the present study, optimized at the GVVPT2 level using the {4}{5} model space and the cc-pVDZ basis set, are given in Table 3. As mentioned above, the most important excitations leading to the states should be localized within the CN_2 fragment and should retain the diazirine ring moiety but with larger N−N bond length. This is confirmed by the data of Table 3. Although the table shows quite varied geometrical parameters for the different states, all of the variations can be understood by analyzing the electronic structures of the states.

The electronic structures of the 1^1B_1 and 1^3B_1 states are predicted to be quite similar. The leading excitation connecting $\tilde{X}^1A_1$ with these states is the $4b_2 \Rightarrow 2a_2$ one-electron excitation. The amplitude of this excitation in 1^1B_1 is 0.82. The second-largest amplitude (0.21) is connected with the two-electron excitation $9a_14b_2 \Rightarrow 10a_12a_2$, and the third (0.19) is $(4b_2)^2 \Rightarrow (2a_2)^1(5b_2)^1$. In the case of 1^3B_1, these excitations have almost the same amplitudes, 0.83, 0.22, and 0.18, respectively, but there is one more large amplitude configuration (0.15), which corresponds to the $5b_14b_2 \Rightarrow 2a_26b_1$ double excitation. Qualitatively, the leading excitation, $4b_2 \Rightarrow 2a_2$, corresponds to an excitation from the antisymmetric, banana-type, three-center N−C−N bonding orbital ($4b_2$) to the π-antibonding N−N orbital ($2a_2$). As seen from Table 3 (and as should be expected), such a single excitation retains the CN_2 ring and leads to increasing the N−N and C−N bond lengths. Displacement of electron density from the carbon atom to the nitrogen atoms, as a result of the excitation, causes displacement of density from the fluorine atoms to carbon and in the shortening of R_{CF}. One should expect an essential change in the dipole moment of the molecule, which is in agreement with the experimental observation of a high intensity $\tilde{A}^1B_1 \leftarrow \tilde{X}^1A_1$ transition ($1^1B_1 \equiv \tilde{A}^1B_1$).

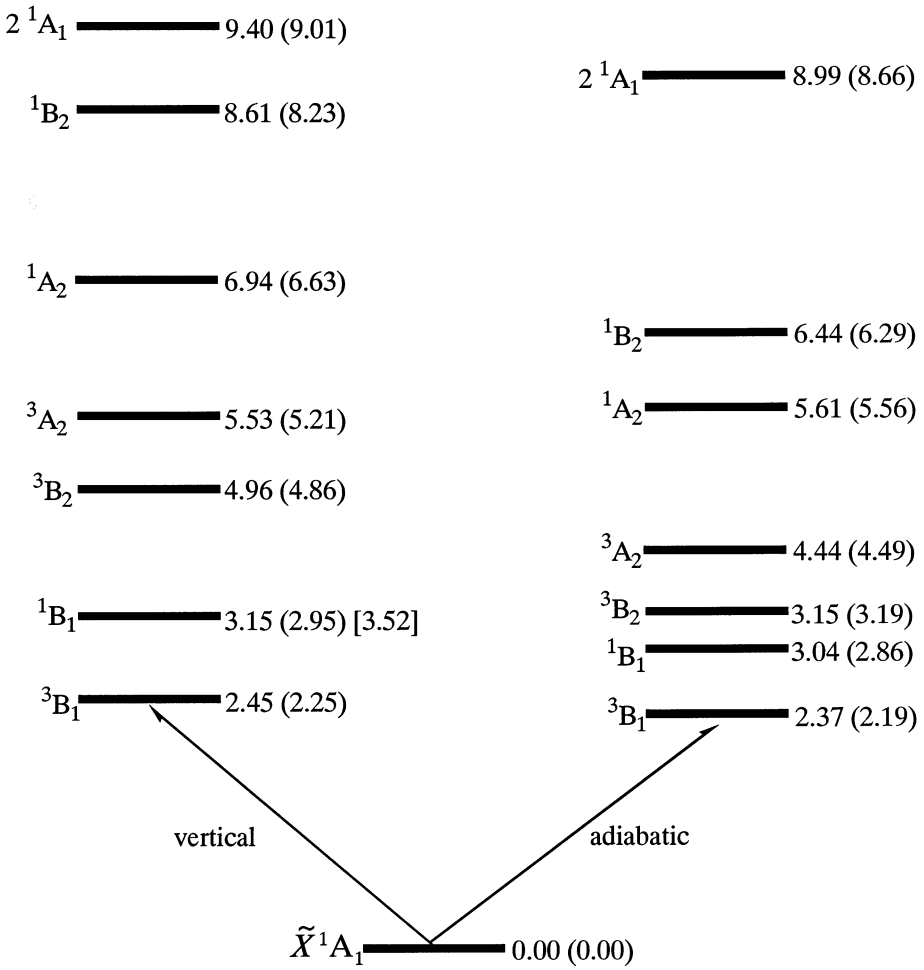

Figure 1. GVVPT2 vertical and adiabatic excitation energies (eV) of excited states of F_2CN_2, calculated with cc-pVDZ and cc-pVTZ (in parentheses) basis sets. Experimental data,[12,15] where available, is given in square brackets.

Our GVVPT2 calculations predict that, as a result of this excitation, the lengths of the N−N and F−F distances should increase and decrease, by +0.031 and −0.037 Å, respectively. These calculated results agree well with the changes of the bond lengths (+0.038 Å for R_{NN} and −0.041 Å for R_{FF}) found in 1990 by Sieber et al.[15] on the basis of analysis of the two-photon excitation spectrum of the molecule.

The electronic structures of the 1^1A_2 and 1^3A_2 states are also similar. Specifically, the triplet has the following four excitations with largest amplitudes: $9a_1 \Rightarrow 2a_2$ (0.82), $9a_14b_2 \Rightarrow 2a_25b_2$ (0.22), $8a_19a_1 \Rightarrow 10a_12a_2$ (0.17), and $9a_15b_1 \Rightarrow 2a_26b_1$ (0.17). The 1^1A_2 singlet state involves these excitations with almost the same amplitudes (0.82, 0.21, 0.16, and 0.15, respectively) but additionally has three more configurations with amplitudes of about 0.10. The leading excitation in both states is the one-electron excitation from the symmetric three-center C−N_2 bonding orbital ($9a_1$) to the π-antibonding N−N orbital ($2a_2$). The other excitations also lead to occupation of the antibonding $2a_2$ orbital. All of these excitations contribute to significantly increasing R_{NN} (by 0.3−0.4 Å) and ∠NCN (by 13−19°) compared to the ground state (cf. Tables 2 and 3).

Among the studied excited states, the electronic nature of the 1^1B_2 singlet state proves to be most complex, and the list of its leading configurations differs significantly from that of the triplet, 1^3B_2. Specifically, the triplet has three leading configurations: $5b_1 \Rightarrow 2a_2$ (0.82), $5b_14b_2 \Rightarrow 2a_25b_2$ (0.26), and $9a_15b_1 \Rightarrow 10a_12a_2$ (0.19), while all other configurations have small amplitudes (<0.10). The 1^1B_2 singlet state involves the same most important configuration ($5b_1 \Rightarrow 2a_2$) but with an essentially smaller amplitude (i.e. only 0.67), but the remaining configurations with largest amplitude are absolutely different: $9a_1 \Rightarrow 5b_2$ (0.46), $5b_14b_2 \Rightarrow 2a_26b_2$ (0.16), $(5b_1)^2 \Rightarrow 2a_26b_1$ (0.15), $8a_15b_1 \Rightarrow 10a_12a_2$ (0.14), and $9a_14b_2 \Rightarrow 5b_26b_2$ (0.13). In both cases, the one-electron excitation from the π-bonding N−N orbital ($5b_1$) to the π-antibonding N−N orbital ($2a_2$) will lead to increasing R_{NN}. However, in the case of the singlet, the $8a_15b_1 \Rightarrow 10a_12a_2$ and $9a_14b_2 \Rightarrow 5b_26b_2$ excitations will increase R_{NN} further because they weaken the strongest σ bond in the N_2 fragment (i.e., through an excitation from the σ-bonding orbital ($8a_1$) and occupation of the σ-antibonding orbital ($6b_2$)). This analysis agrees with the data of Table 3, which shows that the length of the N−N bond in 1^1B_2 is the largest one (1.75 Å) among all the studied excited states and is larger than in 1^3B_2 by about 0.1 Å. Such a large increase of the N−N bond length in 1^1B_2 (by 0.45 Å relative to the ground state) results in a remarkable increase of the N−C−N angle (by +23°). The configuration with the second largest amplitude ($9a_1 \Rightarrow 5b_2$, 0.46) corresponds to an excitation from the C−N_2 orbital to the antibonding, banana-type, N−C−N orbital, which is consistent with the change in molecular structure already noted. None of these excitations should change the dipole moment of the molecule significantly and, as a consequence, should lead to low intensity for the symmetry-allowed $1^1B_2 \leftarrow \tilde{X}^1A_1$ transition (in fact, this transition has not been detected yet).

In contrast to the $1^{1,3}B_2$ states, the second singlet of A_1 symmetry has the simplest configuration structure. The leading

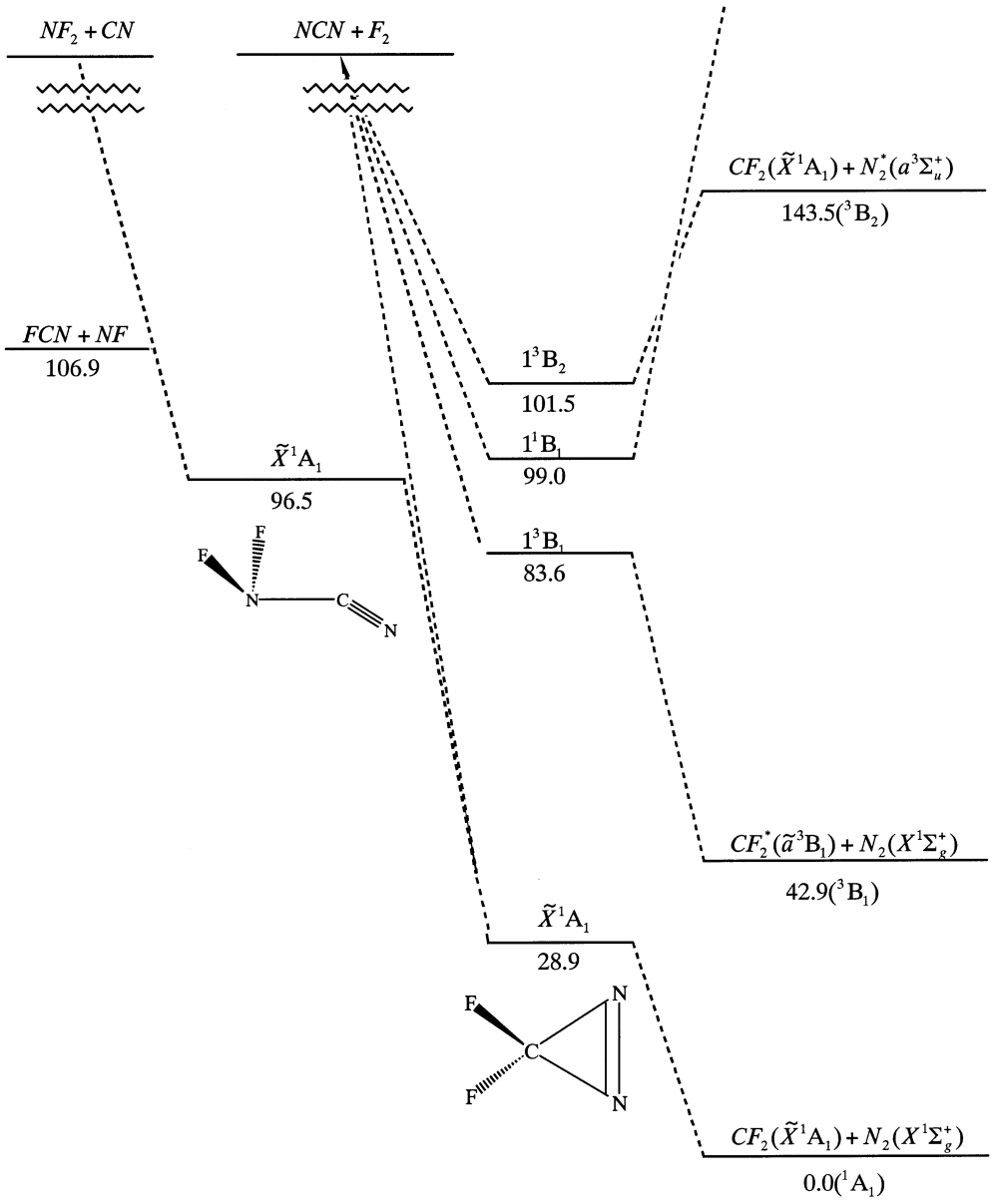

Figure 2. Schematic representation of the relative energies (kcal/mol) of the F_2CN_2 ground and lowest excited states correlating with several of the lowest dissociation limits of the molecule.

excitation in 2^1A_1 is the $(4b_2)^2 \Rightarrow (2a_2)^2$ excitation with an amplitude of 0.87, which qualitatively corresponds to an excitation of two electrons from the banana-type, antisymmetric N−C−N bonding orbital ($4b_2$) to the π-antibonding N−N orbital ($2a_2$). (The corresponding single excitation occurs in $1^{1,3}B_1$ states.) The second-largest amplitude (0.22) in 2^1A_1 is connected with the excitation $(9a_1)^2 \Rightarrow (2a_2)^2$ of two electrons from the bonding C−N_2 orbital to $2a_2$. As should be expected, and as seen in Table 3, these excitations lead first of all to increasing the N−N bond length (by 0.12 Å).

The vertical and adiabatic excitation energies of the considered states, calculated at the GVVPT2 level with cc-pVDZ and cc-pVTZ basis sets, are given in Figure 1. As seen from the figure, results of the calculations are comparatively insensitive to basis set. The lowest-lying excited state of the molecule is predicted to be the 1^3B_1 triplet state, followed by 1^1B_1. The energy of the lowest symmetry-allowed transition $1^1B_1 \leftarrow \tilde{X}^1A_1$ is equal to 3.15 eV (2.95 eV with cc-pVTZ), which agrees reasonably well with the experimental value of 3.52 eV (28 374.2 cm^{-1}).[12,15] The calculated adiabatic excitation energy of 1^1B_1 relative to 1^3B_1 is predicted to be 0.67 eV (with both cc-pVDZ and cc-pVTZ basis sets), which is also relatively close to the value of 0.89 eV (7 200 cm^{-1}), evaluated by Lombardi et al.[11]

The thermodynamic stabilities of the lowest electronic states of difluorodiazirine have been evaluated using (1) experimental data for dissociation limits from JANAF tables,[32] (2) GVVPT2/cc-pVDZ adiabatic excitation energies (as given in Figure 1), and (3) the energy of the ground state (28.9 kcal/mol) relative to the lowest $CF_2 + N_2$ asymptote, calculated in ref 2. The obtained relative energies of the lowest dissociation limits of the molecule and its lowest states that correlate adiabatically with the limits are represented schematically in Figure 2. As seen from the figure and as assumed in ref 16, the 1^1B_1 state is a bound electronic state and hence can predissociate only by coupling to lower-lying states. Our calculations show that there are only two such states, $\tilde{X}^1A_1$ and 1^3B_1; the triplet, 1^3B_1, is found to be metastable (by about 41 kcal/mol) relative to decay into CF_2 (in its $\tilde{a}^3B_1$ lowest excited state) and N_2 (in its ground state). Near the minimum of the 1^1B_1 potential-energy surface, the 1^3B_1 and 1^1B_1 surfaces are separated by about 0.7 eV, and hence the $1^1B_1-1^3B_1$ coupling hardly can explain the observed

slow predissociation of 1^1B_1 in its 0° level. It is thought that, in this case, coupling to highly excited (bound) vibrations of the ground state is the dominant process for the dissociation.[14−16] However, on the basis of our results, one cannot exclude the possibility that the $1^1B_1-1^3B_1$ coupling plays a role in the region of the potential barrier of the 1^3B_1 state. Such coupling would also explain (at least qualitatively) the observed increasing dissociation rate with increasing excitation energy and the fact that, for excitation energies higher than 31 280 cm^{-1}, no fluorescence was observed at all.[14] Such threshold would correspond to a barrier in 1^3B_1 of about 28.8 kcal/mol. These speculations about the possible role of the singlet−triplet coupling in the predissociation of the 1^1B_1 state call for additional studies.

4. Conclusions

In the present work, GVVPT2 calculations, with cc-pVDZ and cc-pVTZ basis sets, have been performed to investigate the equilibrium geometries, thermodynamic stabilities, and vertical and adiabatic excitation energies of the lowest singlet and triplet states of each symmetry of the difluorodiazirine molecule. It has been demonstrated that, although all of the states have essentially multiconfigurational nature (especially the excited ones), the GVVPT2 method addressed all states of interest without any unusual mathematical or computational difficulties. MP2 and QCISD encounter serious difficulties in describing key parameters, such as the C−N bond length, even for the ground state, where the methods might be expected to be applicable. GVVPT2 results for the ground state are similar to, but closer to experiment than, the CCSD(T) results. These results and reported calculations with a variety of model spaces show that a balanced treatment of nondynamic and dynamic correlation effects is of crucial importance for a correct description of the system.

All the studied states are predicted to retain the CN_2 ring but to have significantly longer N−N bonds than the ground state. The calculated structural characteristics of the molecule in its ground ($\tilde{X}^1A_1$) and lowest singlet (1^1B_1) states, as well as the excitation energies of the 1^1B_1 and 1^3B_1 states, are in good agreement with the available experimental structural and spectroscopic data. The performed analysis of the thermodynamic stabilities of the states has shown that there are only two states, $\tilde{X}^1A_1$ and 1^3B_1, lying lower than the predissociating 1^1B_1 state. Our calculations are the first to show that the 1^3B_1 triplet state of the molecule is also metastable, as is the ground state, relative to decay into $CF_2 + N_2$ (by about 41 kcal/mol). This result is likely to be important in fully describing the mechanism of the ultraviolet photolysis of difluorodiazirine.

Acknowledgment. The authors gratefully acknowledge the NSF for financial support of the work presented herein (Grant No. CHE-9975429).

References and Notes

(1) Moffat, J. B. *J. Mol. Struct.* **1979**, *52*, 275.
(2) Boldyrev, A. I.; Schleyer, P. v. R.; Higgins, D.; Thomson, C.; Kramarenko, S. S. *J. Comput. Chem.* **1992**, *13*, 1066.
(3) Sieber, H.; Neusser, H. J.; Stroh, F.; Winnewisser, M. *J. Mol. Spectrosc.* **1991**, *148*, 453.
(4) Burkholder, D.; Jones, W. E.; Ling, K. W.; Wasson, J. S. *Theor. Chim. Acta* **1980**, *55*, 325.
(5) Mitsch, R. A. *J. Heterocycl. Chem.* **1964**, *1*, 59.
(6) Mitsch, R. A. *J. Am. Chem. Soc.* **1965**, *87*, 758.
(7) Mitsch, R. A.; Neuvar, E. W.; Ogden, P. H. *J. Heterocycl. Chem.* **1967**, *4*, 389.
(8) Hencher, J. L.; Bauer, S. H. *J. Am. Chem. Soc.* **1967**, *89*, 5527.
(9) Herr, K. C.; Pimentel, G. C. *Appl. Opt.* **1965**, *4*, 25.
(10) Milligan, D. E.; Mann, D. E.; Jacox, M. E.; Mitsch, R. A. *J. Chem. Phys.* **1964**, *41*, 1199.
(11) Lombardi, J. R.; Klemperer, W.; Robin, M. B.; Basch, H.; Kuebler, N. A., Jr. *Chem. Phys.* **1969**, *51*, 33.
(12) Hepburn, P. H.; Hollas, J. M. *J. Mol. Spectrosc.* **1974**, *50*, 126.
(13) Vandersall, M.; Rice, S. A. *J. Chem. Phys.* **1983**, *79*, 4845.
(14) Sieber, H.; Bruno, A. E.; Neusser, H. J. *J. Phys. Chem.* **1990**, *94*, 203.
(15) Sieber, H.; Riedle, E.; Neusser, H. J. *Chem. Phys. Lett.* **1990**, *169*, 191.
(16) Sieber, H.; Moomaw, W. R.; Neusser, H. J.; Schlag, E. W. *J. Phys. Chem.* **1991**, *95*, 6958.
(17) Simmons, J. D.; Bartky, I. R.; Bass, A. M. *J. Mol. Spectrosc.* **1965**, *17*, 48.
(18) Bjork, C. W.; Craig, N. C.; Mitsch, R. A.; Overend, J. *J. Am. Chem. Soc.* **1965**, *87*, 1186.
(19) Craig, N. C.; Kliewer, M. A. *Spectrochim. Acta, Part A* **1979**, *35A*, 895.
(20) Meyers, M. D.; Frank, S. *Inorg. Chem.* **1966**, *5*, 1455.
(21) Pandey, R. R.; Khait, Y. G.; Hoffmann, M. R. *THEOCHEM* **2001**, *542*, 177.
(22) Song, J.; Khait, Y. G.; Wang, H.; Hoffmann, M. R. *J. Chem. Phys.* **2003**, *118*, 10065.
(23) Kraka, E.; Konkoli, Z.; Cremer, D.; Fowler, J.; Schaefer, H. F., III. *J. Am. Chem. Soc.* **1996**, *118*, 10595.
(24) Khait, Y. G.; Song, J.; Hoffmann, M. R. *J. Chem. Phys.* **2002**, *117*, 4133.
(25) Hoffmann, M. R. *Chem. Phys. Lett.* **1993**, *210*, 193.
(26) Hoffmann, M. R. *J. Phys. Chem.* **1996**, *100*, 6125.
(27) Dudley, T. J.; Hoffmann, M. R. *Mol. Phys.* **2003**, *101*, 1303.
(28) Khait, Y. G.; Hoffmann, M. R. *J. Chem. Phys.* **1998**, *108*, 8317.
(29) Khait, Y. G.; Song, J.; Hoffmann, M. R. *Int. J. Quantum Chem*. In press.
(30) Frisch, M. J.; Trucks, G. W.; Schlegel, H. B.; Scuseria, G. E.; Robb, M. A.; Cheeseman, J. R.; Zakrzewski, V. G.; Montgomery, J. A., Jr.; Stratmann, R. E.; Burant, J. C.; Dapprich, S.; Millam, J. M.; Daniels, A. D.; Kudin, K. N.; Strain, M. C.; Farkas, O.; Tomasi, J.; Barone, V.; Cossi, M.; Cammi, R.; Mennucci, B.; Pomelli, C.; Adamo, C.; Clifford, S.; Ochterski, J.; Petersson, G. A.; Ayala, P. Y.; Cui, Q.; Morokuma, K.; Malick, D. K.; Rabuck, A. D.; Raghavachari, K.; Foresman, J. B.; Cioslowski, J.; Ortiz, J. V.; Stefanov, B. B.; Liu, G.; Liashenko, A.; Piskorz, P.; Komaromi, I.; Gomperts, R.; Martin, R. L.; Fox, D. J.; Keith, T.; Al-Laham, M. A.; Peng, C. Y.; Nanayakkara, A.; Gonzalez, C.; Challacombe, M.; Gill, P. M. W.; Johnson, B. G.; Chen, W.; Wong, M. W.; Andres, J. L.; Head-Gordon, M.; Replogle, E. S.; Pople, J. A. *Gaussian 98*; Gaussian, Inc.: Pittsburgh, PA, 1998.
(31) Hoffmann, M. R.; Sherrill, C. D.; Leininger, M. L.; Schaefer, H. F., III. *Chem. Phys. Lett.* **2002**, *355*, 183.
(32) Chase, M. W., Jr.; Davies, C. A.; Downey, J. R., Jr.; Frurip, D. J.; McDonald, R. A.; Syverud, A. N. *JANAF Thermochemical Tables, Third Edition, J. Phys. Chem. Ref. Data Suppl.* **1985**, *14*, 1.